separation of resonances that will allow for the accurate measurement of peak intensities.

Conclusions

We report here the experimental observation of four different configurational isomers for both morphiceptin, Tyr-Pro-Phe-Pro-NH_2, and the (NMe)Phe analogue, Tyr-Pro-(NMe)Phe-D-Pro-NH_2. The four isomers, with small differences in ratio of configurational populations, were observed in both water and DMSO. Using ^1H and ^{13}C NMR the unambiguous assignment of the two major isomers for each compound was carried out. The results presented clearly indicate the importance of exploring all possible isomers when examining a peptide containing an internal or C-terminal proline or *N*-methyl-substituted residue. The all-trans structures for morphiceptin and the (NMe)Phe analogue, comprising 60% and 55%, respectively, may only represent a part of the biological profile for these peptidic opiates. We are continuing our studies on the conformations and possible separations of these stereoisomers in order to develop structure–biological activity relationships.

Acknowledgment. The authors gratefully acknowledge NIH Grant DK1540, which helped support this research.

Registry No. H-Tyr-Pro-Phe-Pro-NH_2, 74135-04-9; H-Tyr-Pro-(NMe)Phe-D-Pro-NH_2, 83397-56-2.

Vibrational Spectra and Normal Mode Analysis for [2Fe–2S] Protein Analogues Using ^{34}S, ^{54}Fe, and ^2H Substitution: Coupling of Fe–S Stretching and S–C–C Bending Modes

Sanghwa Han, Roman S. Czernuszewicz, and Thomas G. Spiro*

Contribution from the Department of Chemistry, Princeton University, Princeton, New Jersey 08544. *Received May 23, 1988*

Abstract: Resonance Raman (RR) and infrared (IR) spectra are reported for analogue complexes of Fe_2S_2 proteins: $[(C_2H_5)_4N]_2[Fe_2S_2(SCH_3)_4]$, $[(n\text{-}C_3H_7)_4N]_2[Fe_2S_2(SC_2H_5)_4]$, and $[(C_2H_5)_4N]_2[Fe_2S_2(S_2\text{-}o\text{-}xyl)_2]$ (S_2-o-xyl = *o*-xylene-α,α'-dithiolate) and their isotopomers with ^{34}S at the bridging positions. For the xylenedithiolate complex the effects of substituting ^{54}Fe, ^{34}S at the terminal positions and ^2H at the methylene positions were also investigated. All eight Fe–S stretching modes have been assigned via their RR and IR activities and their isotope shifts. In addition a S–C–C bending mode has been identified in RR spectra of the ethanethiolate and xylenedithiolate complexes through its interaction with a nearly coincident Fe–S stretching mode. The frequencies and isotope shifts were calculated using a $Fe_2S_2(SC_2H_5)_4$ model with point mass methyl and methylene groups and structural parameters of the *o*-xylenedithiolate complex. This model was used to gauge the sensitivity of the vibrational frequencies to the Fe–S–C–C dihedral angle, τ; as τ increases from 90°, four of the Fe–S stretching modes increase, while one decreases, owing to differential couplings with the S–C–C bending coordinates. The lowest frequency Fe–S stretching mode, at $\sim$275 cm^{-1}, is an IR-active out-of-phase breathing mode of the two linked FeS_4 tetrahedra. In the xylenedithiolate and ethanethiolate complexes, but not in the methanethiolate complex, this mode also shows significant RR activation, with an even stronger RR overtone band. This behavior is attributed to unusual sensitivity of this mode to environmental asymmetry, resulting in a significant excited-state origin shift and force constant change. RR intensities of other combination tones suggest excited-state Duschinsky rotation among the interacting S–C–C bending and Fe–S stretching modes. A band of variable intensity at $\sim$200 cm^{-1} is assigned to a mode involving mutual displacement of the Fe atoms; its large intensity for the xylenedithiolate complex suggests appreciable direct interaction of the Fe orbitals. RR bands in the 120–150-cm^{-1} region are assigned to S–Fe–S bending modes.

As part of a program of resonance Raman (RR) spectroscopic studies of iron–sulfur proteins and their small molecule analogues,[1] we present vibrational analyses of $[Fe_2S_2(SR)_4]^{2-}$ complexes, analogues of the Fe_2S_2 proteins. These complexes, first prepared in the pioneering synthetic program of Holm and co-workers,[2] have played a key role in the elucidation of the protein active sites, providing accurate structures against which various spectroscopic signatures can be compared. The first such Fe_2S_2 analogue, and the most stable one, contains the chelating ligand *o*-xylene-α,α'-dithiolate (S_2-o-xyl), used by Holm and colleagues to prevent further oligomerization of the Fe_2S_2 centers.[3]

The xylenedithiolate analogue served as the basis for a previous RR analysis of Fe_2S_2 proteins from this laboratory, using ^{34}S labeling of the labile (bridging) sulfur atoms in the proteins.[4] Isotopes were unavailable for the analogue, however, whose RR spectrum differs in significant details from those of the proteins. Moreover, the spectral quality, while significantly better than had been reported in previous studies,[5-7] left room for improvement. We now report higher quality RR, and also IR, spectra of the xylenedithiolate analogue, obtained at low temperature (77 K) in pressed KBr pellets of the tetraethylammonium salt. These data reveal new spectral features. We have also determined the effects on the spectra of isotope substitution at Fe, bridging S, terminal S, and methylene H. The isotope shifts provide secure assignments of all eight Fe–S stretching modes, some of which differ from those previously suggested. In addition there is unambiguous evidence for interaction of S–C–C bending with two of the Fe–S stretching modes.

* Author to whom correspondence should be addressed.

(1) Spiro, T. G.; Czernuszewicz, R. S.; Han, S. In *Biological Applications of Raman Spectroscopy*; Spiro, T. G., Ed.; Wiley-Interscience: New York, 1988; Vol. III, Chapter 12.
(2) Berg, J. M.; Holm, R. H. In *Iron-Sulfur Proteins*; Spiro, T. G., Ed.; Wiley-Interscience: New York, 1982; Chapter 1.
(3) Mayerle, J. J.; Denmark, S. E.; DePamphilis, B. V.; Ibers, J. A.; Holm, R. H. *J. Am. Chem. Soc.* **1975**, *97*, 1032–1045.
(4) Yachandra, V. K.; Hare, J.; Gewirth, A.; Czernuszewicz, R. S.; Kimura, T.; Holm, R. H.; Spiro, T. G. *J. Am. Chem. Soc.* **1983**, *105*, 6462–6468.
(5) Tang, S.-P. W.; Spiro, T. G.; Mukai, K.; Kimura, T. *Biochem. Biophys. Res. Commun.* **1973**, *53*, 869–874.
(6) Adar, F.; Blum, H.; Leigh, J. S., Jr.; Ohnishi, T.; Salerno, J.; Kimura, T. *FEBS Lett.* **1977**, *84*, 214–216.
(7) Blum, H.; Adar, F.; Salerno, J. C.; Leigh, J. S., Jr. *Biochem. Biophys. Res. Commun.* **1977**, *77*, 650–657.

0002-7863/89/1511-3496$01.50/0

The observed band frequencies and isotope shifts are quantitatively reproduced with a normal coordinate calculation via a physically reasonable force field and a simplified molecular model incorporating the $Fe_2S_2(SCC)_4$ structure parameters of the xylenedithiolate complex. This model has been used to anticipate the effects of conformational change involving rotations about the S–C bonds, which are calculated to influence several Fe–S stretching frequencies significantly. In the following paper,[8] these findings are used in reanalyzing Fe_2S_2 protein RR spectra. The normal mode analysis provides a satisfying insight into the nature of the lowest frequency Fe–S stretching mode, which is weak or absent in analogue RR spectra but is one of the strongest protein bands.

The xylenedithiolate analogue data are supplemented with RR and IR spectra of Fe_2S_2 analogues with methanethiolate and ethanethiolate ligands. These complexes are relatively unstable and their vibrational spectra have not previously been reported. Our recently developed synthetic route[9] has permitted preparation of pure samples and the incorporation of ^{34}S into the bridging positions. The importance of these species is that they represent the simplest analogues with and without the critical S–C–C bending coordinate. Their spectra and isotope shifts are fully consistent with the interpretation of the xylenedithiolate analogue data.

We note that Beardwood and Gibson[10] have reported IR and RR spectra of some Fe_2S_2 analogues and suggested assignments based on spectral changes associated with replacement of the bridging S atoms with Se. This method, however, suffers from introducing too large a perturbation. The doubling of the bridging atom masses changes the mode compositions and makes correlations difficult. Using ^{34}S, one can be confident that the mode character is not significantly altered by the substitution.

Experimental Section

All the analogue complexes were prepared by the synthetic procedure described in ref 9. Elemental ^{34}S (95% enriched, Oakridge National Laboratories) was used for labeling the bridging position. The xylenedithiolate complex with terminal ^{34}S was prepared by using $(H^{34}S)_2$-o-xyl,[3] which was obtained from the reaction of α,α'-dibromo-o-xylene with [^{34}S]thiourea (93% enriched, ICON Services, Summit, N.J.). The methylene deuterated complex was prepared from the corresponding 1-Fe complex.[11] ^{54}Fe substitution was carried out by using anhydrous $^{54}FeCl_3$ as the starting material, which was prepared via reaction of $^{54}Fe_2O_3$ (97% enriched, Oakridge) with thionyl chloride in a sealed tube.[12] Purity of the complexes was checked by UV–vis spectra and elemental analyses.

RR spectra were collected in a backscattering geometry from KBr pellets attached anaerobically to a cold tip cooled with liquid nitrogen.[13] This technique not only improves resolution due to the low temperature but also eliminates interference from glass or quartz Raman bands, which fall in the Fe–S stretching frequency region, since the glass enclosure is distant from the sample surface upon which the laser is focused. Samples were stable under prolonged laser irradiation at 568.2 or 647.1 nm, but significant photodecomposition was observed when shorter wavelengths were used.

Excitation lines were provided by Spectra Physics 171 Kr^+ and 2025 Ar^+ lasers. The laser power at the sample was typically 150 mW. The scattered light was dispersed with a Spex 1402 double monochromator and detected by a cooled RCA 31034 photomultiplier tube and an ORTEC 9315 photon counting system under the control of a MINC II (DEC) minicomputer. Infrared spectra were recorded on a Digilab FT20C Fourier-transform infrared spectrophotometer equipped with a N_2 purge sample chamber. The IR spectra were run in Nujol mulls in the same cell used for Raman experiments except that polyethylene windows were attached for far-IR transparency. The Raman spectra shown in the figures are typically the sum of 8 to 10 scans with 0.5- or 0.2-cm^{-1}/s increments.

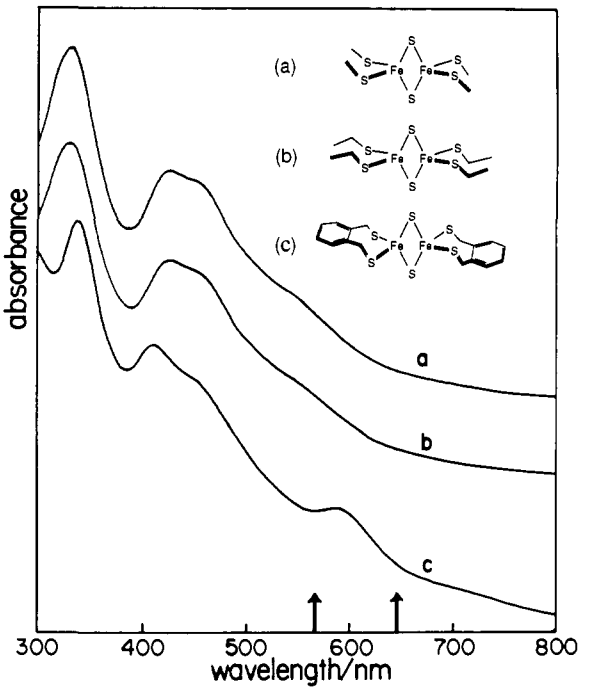

Figure 1. Absorption spectra of Fe_2S_2 complexes in dimethylformamide: (a) $(Et_4N)_2[Fe_2S_2(SCH_3)_4]$; (b) $(Pr_4N)_2[Fe_2S_2(SC_2H_5)_4]$; (c) $(Et_4N)_2[Fe_2S_2(S_2\text{-o-xyl})_2]$. Arrows mark the Raman excitation wavelengths.

Normal mode calculations were performed by using the GF matrix method.[14] Schachtschneider's programs[15] were used for constructing G matrices and solving the secular equations.

Results and Discussion

The three analogue complexes $(Et_4N)_2[Fe_2S_2(SCH_3)_4]$, $(Pr_4N)_2[Fe_2S_2(SCH_2CH_3)_4]$, and $(Et_4N)_2[Fe_2S_2(S_2\text{-o-xyl})_2]$ (Et_4N^+ and Pr_4N^+ are tetraethyl- and tetrapropylammonium counterions) were chosen for the following reasons. The methanethiolate complex is the simplest analogue containing a S–C bond, and should give the simplest vibrational spectrum. The ethanethiolate complex is the simplest analogue containing the SCC unit, whose bending coordinate turns out to be an important contributor to the vibrational spectrum. The xylenedithiolate complex is important because its high-resolution X-ray crystal structure is available.[3] In addition the xylenedithiolate chelate ring fixes the SCC unit in a defined orientation, a key requirement in the vibrational analysis. The xylenedithiolate complex is easy to prepare[3,9] and the ligand is amenable to ^{34}S substitution[9] and to deuteration at the methylene carbon atom.[11] These modifications give valuable isotope shift information. The methanethiolate and ethanethiolate analogues are less stable than the xylenedithiolate analogue, but they have recently been prepared in pure form using a method that permits convenient ^{34}S substitution.[9]

1. Spectra. Figure 1 shows absorption spectra of the three Fe_2S_2 complexes included in this study. They have broad, weakly structured absorption, rising throughout the visible region, to a peak at ~410 nm. These spectra arise from numerous overlapping S–Fe charge-transfer (CT) transitions.[16] It is interesting that only the xylenedithiolate complex shows a distinct band at ~600 nm, perhaps reflecting the effect of the constraining xylenedithiolate chelate ring on the CT transition moments and/or energies. The S → Fe CT transitions are expected and observed[1] to be effective in enhancing Raman bands associated with the stretching of the Fe–S bonds. The Raman excitation wavelengths, 568.2 and 647.1 nm, are marked with arrows. Although shorter

(8) Han, S.; Czernuszewicz, R. S.; Kimura, T.; Adams, M. W. W.; Spiro, T. G. *J. Am. Chem. Soc.*, following paper in this issue.
(9) Han, S.; Czernuszewicz, R. S.; Spiro, T. G. *Inorg. Chem.* **1986**, *25*, 2276–2277.
(10) Beardwood, P.; Gibson, J. F. *J. Chem. Soc., Dalton Trans.* **1984**, 1507–1516.
(11) Yachandra, V. K.; Hare, J.; Moura, I.; Spiro, T. G. *J. Am. Chem. Soc.* **1983**, *105*, 6455–6461.
(12) North, H. B.; Hageman, A. M. *J. Am. Chem. Soc.* **1913**, *35*, 352–356.
(13) Czernuszewicz, R. S.; Johnson, M. K. *Appl. Spectrosc.* **1983**, *37*, 297–298.
(14) Wilson, E. B., Jr.; Decius, J. C.; Cross, P. C. *Molecular Vibrations*; Dover Publishing: New York, 1980.
(15) Schachtschneider, J. H. Shell Development Co., Technical Report No. 263-62, 1962.
(16) Noodleman, L.; Case, D. A.; Aizman, A. *J. Am. Chem. Soc.* **1988**, *110*, 1001–1005 and references therein.

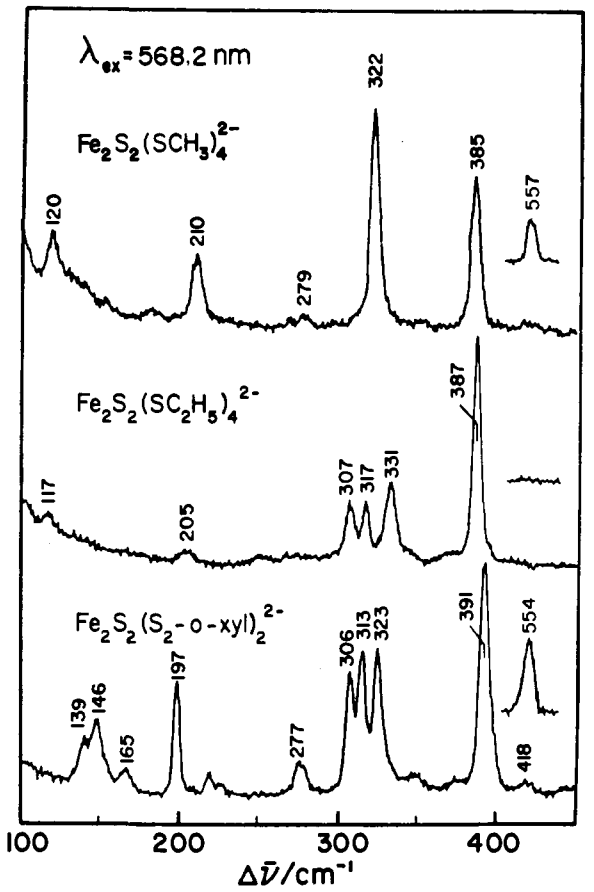

Figure 2. Resonance Raman spectra of Fe_2S_2 complexes as R_4N^+ salts (R = ethyl for SCH_3 and S_2-o-xyl complexes, and *n*-propyl for the SC_2H_5 complex) in KBr pellets obtained via backscattering from a liquid N_2 Dewar,[13] using 568.2-nm Kr^+ laser excitation (150 mW) and 4-cm^{-1} slit widths. The insets are the overtone bands of the ~278-cm^{-1} fundamental, shown on the same intensity scale.

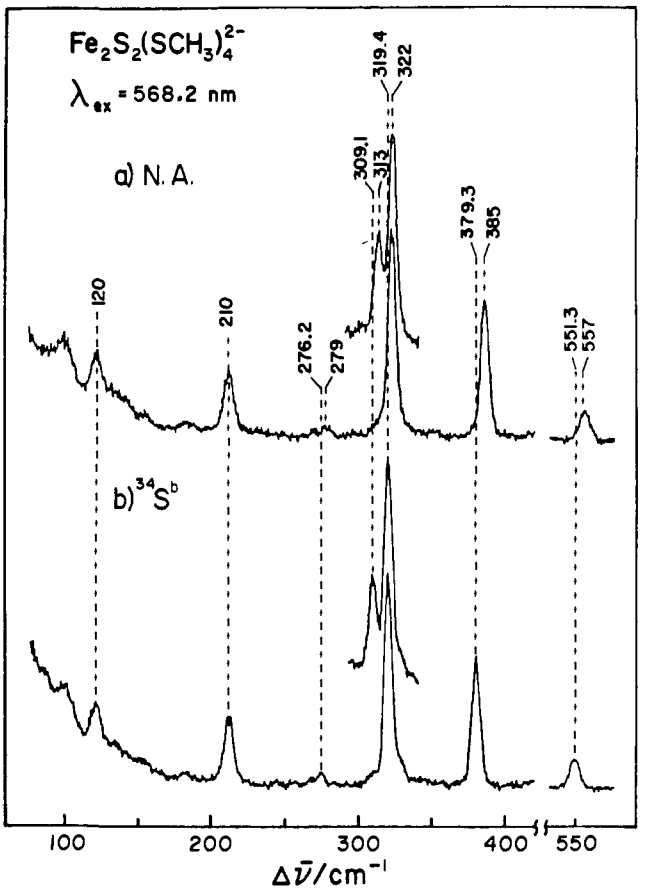

Figure 3. Resonance Raman spectra (77 K, KBr pellet) of $(Et_4N)_2[Fe_2S_2(SCH_3)_4]$: (a) natural abundance (N.A.) and (b) with ^{34}S substituted at the bridging positions ($^{34}S^b$). Conditions: 568.2-nm excitation, 4-cm^{-1} slit widths, 0.5-cm^{-1} increments. The insets are traces with 647.1-nm excitation, showing an extra $^{34}S^b$-sensitive band at 313 cm^{-1}.

wavelengths are known to give stronger resonance enhancement in Fe_2S_2 proteins, they produce photodecomposition of the analogues, particularly of the ethanethiolate and the methanethiolate complexes. Consequently the present study was limited to longer wavelengths. Excitation profiles of Fe_2S_2 proteins are presented and discussed in the succeeding paper.[8]

Figure 2 compares 568.2-nm excited RR spectra of the three analogue complexes in the 100–450-cm^{-1} region, while Figures 3, 4, and 5 show the effect of ^{34}S substitution on these spectra. For the xylenedithiolate complex ^{34}S was substituted for the terminal (S^t) as well as the bridging (S^b) sulfur atoms. Figure 6 shows a high-sensitivity scan of the 500–800-cm^{-1} region of the xylenedithiolate RR spectra, where several overtone and combination bands are found. Figure 7 shows the effect on a critical region of the xylenedithiolate RR spectrum of deuteration at the methylene positions (d_8). Figure 8 shows the IR spectra of the three analogue complexes in the 200–450-cm^{-1} region.

2. Normal Coordinate Analysis. A normal coordinate analysis was carried out to aid in the mode assignments and to develop a reliable FeS force field. These calculations update those of Yachandra et al.[4] by taking advantage of the better resolved spectra and more complete isotope data available in the present study. As in the earlier analysis,[4] a $Fe_2S_2(SCH_2CH_3)_4$ model was adopted, with point mass methyl and methylene groups, and average bond distances and angles taken from the crystal structure of $(Et_4N)_2[Fe_2S_2(S_2\text{-o-xyl})_2]$.[3] The $Fe_2S_2{}^bS_4{}^t$ core of the model was constrained to have D_{2h} symmetry while the ethyl groups were oriented to maintain overall C_{2h} symmetry, with 90° Fe–S–C–C dihedral angles, consistent with the xylenedithiolate analogue crystal structure.

Table I lists the force constants. As before,[4] a Urey–Bradley force field was employed, but this time modified to include nonzero

Table I. Force Constants Used for the $Fe_2S_2(SCH_2CH_3)_4$ Normal Mode Calculation[a]

diagonal		off-diagonal	
K(Fe–S^b)	1.37	F(Fe···Fe)	0.19
K(Fe–S^t)	1.14	f(FeS^b/FeS^b)[b]	0.09
K(S–C)	2.50	f(FeS^b/FeS^b)[c]	0.07
K(C–C)	4.80	f(FeS^b/FeS^t)	0.08
H(FeS^bFe)	0.45	f(FeS^t/FeS^t)	0.12
H(S^bFeS^b)	0.40		
H(S^bFeS^t)	0.38		
H(S^tFeS^t)	0.35		
H(FeSC)	0.35		
H(SCC)	0.82		

[a] K = stretching (mdyn/Å); H = bending (mdyn·Å/rad²); F = nonbonded interaction (mdyn/Å); f = stretch–stretch valence interaction (mdyn/Å). S^b and S^t denote bridging and terminal S atoms, respectively. [b] S^b as the common atom. [c] Fe as the common atom.

interaction constants between adjacent Fe–S bond stretching coordinates; without these it was impossible to reproduce the observed isotope shift pattern (i.e., the correct normal mode composition). Intuitively, the S···S nonbonded contacts might be thought to be important determinants of the force field, yet the allowable force constants were previously found to be quite small.[4,17] The S···S force constants were omitted as an unnecessary complication in the present calculation. It is important to include a Fe···Fe nonbonded force constant (present work) or Fe–Fe stretching force constant (previous work[4]) in order to reproduce the isotope shifts with reasonable Fe–S constants. The presence

(17) Czernuszewicz, R. S.; Macor, K. A.; Johnson, M. K.; Gewirth, A.; Spiro, T. G. *J. Am. Chem. Soc.* **1987**, *109*, 7178–7187.

Table II. Calculated Frequencies[a] and Isotope Shifts[b] (cm^{-1}) for the $Fe_2S_2(SCH_2CH_3)_4$ Model[c] and Observed Values for $[Fe_2S_2(S_2\text{-o-xyl})_2]^{2-}$

		$\Delta^{34}S^b$		$\Delta^{34}S^t$		$\Delta^{54}Fe$			
obs	calc	obs	calc	obs	calc	obs	calc	PED (%)[d]	assignment[e]
415[f]	415	6.0	7.1	0.5	0.0	2.8	3.1	b(79) + α(14)	$B_u^b(B_{2u}^b)$
391	390	5.9	5.8	0.5	0.5	2.7	3.1	b(79) + t(17)	$A_g^b(A_g^b)$
342[f]	344	3.2	2.5	2.7	2.2	1.5	1.3	b(44) + t(41)	$B_u^b(B_{3u}^b)$
327[f]	327	0.0	0.1	4.5	4.9	2.5	2.8	t(85)	$A_u^t(B_{1u}^t)$
	324		0.0		5.1		2.7	t(88)	$B_g^t(B_{2g}^t)$
323	323	2.0	3.1	4.1	4.3	1.0	0.9	b(13) + t(52) + α(14) + δ(13)	$A_g^t(A_g^t)$
313	314	3.2	2.0	1.3	1.1	1.7	2.3	b(61) + δ(26)	$A_g^b(B_{1g}^b)$
306	303	2.5	2.2	1.0	2.4	1.0	1.0	b(39) + δ(38)	A_g^{SCC}
276[f]	278	3.2	3.2	5.2	5.1	0.0	0.0	b(32) + t(50)	$B_u^t(B_{3u}^t)$
197	198	1.0	1.0	2.4	2.3	1.5	1.2	α(37) + β(14) + γ(29)	A_g^{Fe-Fe}

[a] Partial list. Excluded from the table are frequencies involving S–C stretching (673 cm^{-1}), C–C stretching (1082 cm^{-1}), Fe–S–C bending (~120 cm^{-1}), and several low-frequency (<160 cm^{-1}) S–Fe–S bending modes. [b] $\Delta^{34}S^b$, $\Delta^{34}S^t$, and $\Delta^{54}Fe$ denote isotope shifts upon ^{34}S substitution at bridging and terminal positions, and ^{54}Fe substitution, respectively. [c] In this model x axis is along the Fe–Fe vector, y axis is along the S–S vector, and z axis is normal to the $Fe_2S_2^b$ plane. [d] Calculated potential energy distribution (%). Stretching coordinates: b = Fe–S^b, t = Fe–S^t; bending coordinates; α = Fe–S^b–Fe, β = S^b–Fe–S^b, γ = Fe–S–C, δ = S–C–C. [e] Symmetry species in the C_{2h} point group; the superscripts indicate the main internal coordinate. Parent symmetries in the D_{2h} point group are given in parentheses for the Fe–S stretching modes. [f] IR frequencies; the remaining data are from RR spectra.

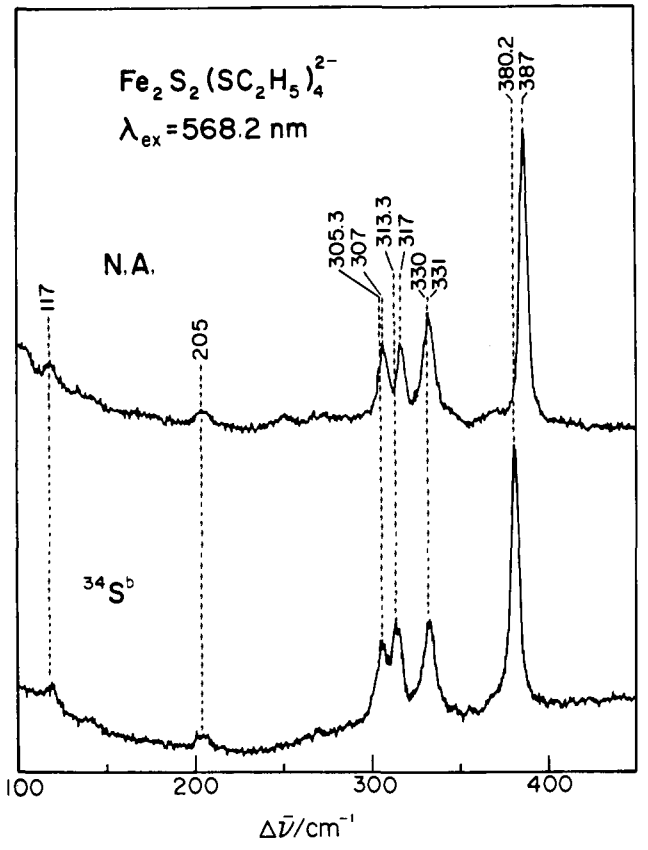

Figure 4. Resonance Raman spectra (77 K, KBr pellet) of $(Pr_4N)_2$-$[Fe_2S_2(SC_2H_5)_4]$: (a) natural abundance (N.A.) and (b) with ^{34}S substituted at the bridging positions. Conditions as in Figure 3.

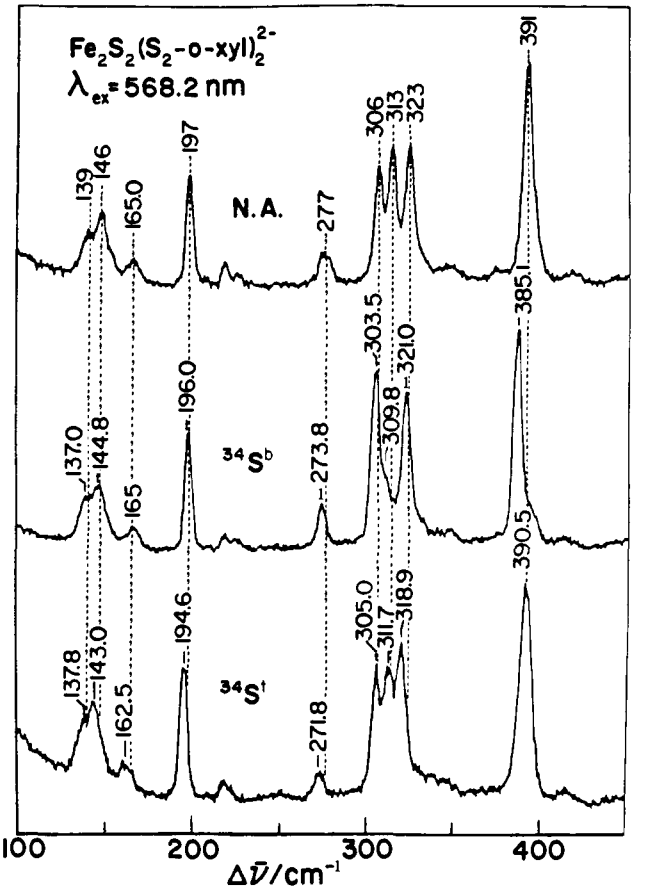

Figure 5. Resonance Raman spectra (77 K, KBr pellet) of $(Et_4N)_2$-$[Fe_2S_2(S_2\text{-o-xyl})_2]$ at natural isotopic abundance (N.A.), and substituted with ^{34}S at the bridging ($^{34}S^b$) and terminal ($^{34}S^t$) positions. Conditions as in Figure 3. For the three closely spaced bands at 306, 313, and 323 cm^{-1}, the isotope shifts were determined from separate scans with 3-cm^{-1} slit widths and 0.2-cm^{-1} increments.

or absence of metal–metal bonding in bridged complexes cannot be determined from a normal coordinate calculation because of cyclic redundancies.[18] The force constants in Table I supercede the ones given in ref 4. We note that bending force constants are higher than in the previous work. These alterations were required in order to get the isotope shifts right, and the new force constants are in line with values reported in the literature.[19,20] Although the higher values represent an appreciable fraction, up to 30%, of the magnitude of the stretching force constants, this is not an unusual situation for metal–ligand bonds.[21]

Calculated frequencies and isotope shifts are compared with those observed for the xylenedithiolate complex in Table II. Table III compares the frequencies of corresponding modes for the three

(18) Bulliner, P. A.; Spiro, T. G. *Spectrochim. Acta* **1970**, *26A*, 1641–1650.
(19) (a) Geetharani, K.; Sathyanarayana, D. N. *Spectrochim. Acta* **1974**, *30A*, 2165–2171. (b) Schlapfer, C. W.; Nakamoto, K. *Inorg. Chem.* **1975**, *14*, 1338–1344.
(20) (a) Scott, D. W.; El-Sabban, M. Z. *J. Mol. Spectrosc.* **1969**, *30*, 317–337. (b) Sugeta, H. *Spectrochim. Acta* **1975**, *31A*, 1729–1737.
(21) Nakamoto, K. *Infrared and Raman Spectra of Inorganic and Coordination Compounds*; Wiley-Interscience: New York, 1986.

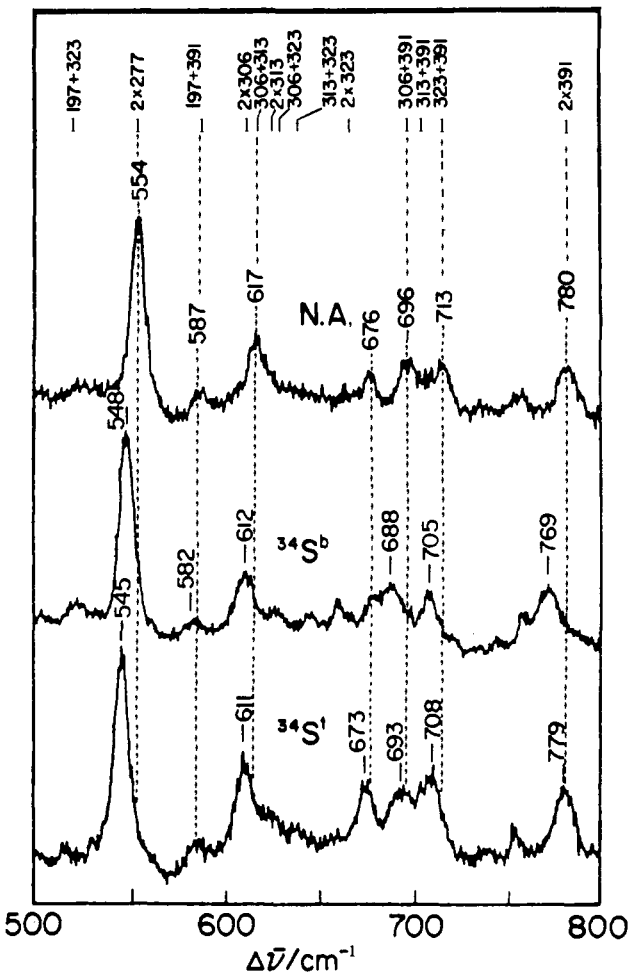

Figure 6. Resonance Raman spectra (77 K, KBr pellet) of $(Et_4N)_2[Fe_2S_2(S_2\text{-o-xyl})_2]$ in the 500–800-cm^{-1} region with 568.2-nm excitation and 8-cm^{-1} slit widths. Marked at the top are the positions of the overtone and combination modes of the 197–391-cm^{-1} fundamentals.

Table III. Mode Frequencies (cm^{-1}) and $^{34}S^{b}$ Isotope Shifts (Parentheses) for the Fe_2S_2 Protein Analogue Complexes

assignment[a]	S_2-o-xyl[b]	SC_2H_5[c]	SCH_3[d]
B_{2u}^{b}	415[e] (6.0)	411[e] (6.2)	409[e] (6.5)
A_g^{b}	391 (5.9)	387 (6.7)	385 (5.7)
B_{3u}^{b}	342[e] (3.2)	345[e] (2.5)	345[e] (3.2)
B_{1u}^{t}	327[e] (0.0)	325[e] (0.3)	329[e] (0.0)
B_{2g}^{t}		326[f] (0.0)	
A_g^{t}	323 (2.0)	331 (1.0)	322 (2.6)
B_{1g}^{b}	313 (3.2)	317 (3.7)	313[f] (3.9)
A_g^{SCC}	306[g] (2.5)	307 (1.7)	
B_{3u}^{t}	276[e] (3.2)	262[e] (2.0)	279[e] (2.8)
A_g^{Fe-Fe}	197 (1.0)	205 (0.0)	210 (0.0)

[a] See Table II; D_{2h} notation used. [b] $(Et_4N)_2[Fe_2S_2(S_2\text{-o-xyl})_2]$; S_2-o-xyl = o-xylene-α,α'-dithiolate. [c] $(Pr_4N)_2[Fe_2S_2(SC_2H_5)_4]$. [d] $(Et_4N)_2[Fe_2S_2(SCH_3)_4]$. [e] IR frequencies; the remainder are RR frequencies. [f] Observed only with 647.1-nm excitation. [g] Other SCC bending modes belong to B_{2g}, B_{1u}, and B_{3u} species in D_{2h} symmetry; not observed in the spectra.

analogue complexes. Not listed are the modes associated with C–C stretching, expected in the ~1000-cm^{-1} region, C–S stretching, expected in the 700-cm^{-1} region (see below), and several bending modes associated with the S–Fe–S angles, calculated below 160 cm^{-1}. Of the four S–C–C bending modes, expected near 300 cm^{-1}, only one has been detected. Figure 9 shows eigenvectors for the assigned modes.

Reference to Table II and Figure 9 will be helpful in the ensuing discussion of the detailed assignments. In this discussion we use point group labels, for either D_{2h} or C_{2h} symmetry point groups

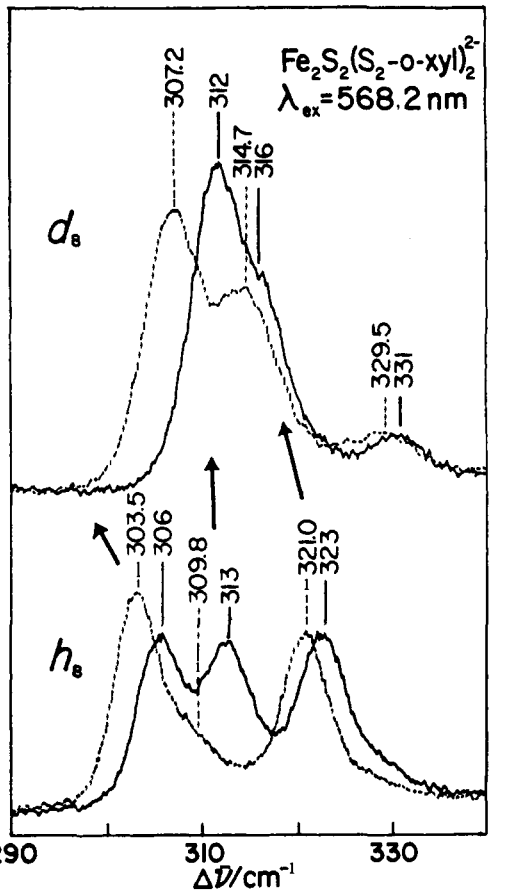

Figure 7. High-resolution (3-cm^{-1} slit widths, 0.2-cm^{-1} increments) Raman scans (568.2-nm excitation) of $(Et_4N)_2[Fe_2S_2(S_2\text{-o-xyl})_2]$ (77 K, KBr pellet), showing changes in the 300–330-cm^{-1} region upon substituting $^{34}S^{b}$ (dashed lines) for $^{32}S^{b}$ (solid lines) in samples containing ^{1}H (h_8) or ^{2}H (d_8) at the methylene carbon atoms of the S_2-o-xyl ligands. The intensities were normalized with respect to the 391-cm^{-1} band (not shown). The arrows show the mode shifts upon deuterium substitution. The position of the 309.8-cm^{-1} band was determined from the 647.1-nm excited spectrum.

as appropriate. In addition the modes are identified by a superscript referring to the main internal coordinate contributor, stretches of the bridging (b) or terminal (t) Fe–S bonds, or of the Fe–Fe bond, or S–C–C bending. These symbols are needed for clarity and conciseness but they should not obscure the fact that there is substantial coordinate mixing in several of the modes, as indicated by the isotope pattern and by the calculated potential energy distributions. For example, the B_u^{b} mode (342 cm^{-1}) has only a slightly larger bridging than terminal ^{34}S isotope shift, and vice versa for the B_u^{t} mode (276 cm^{-1}). Meyer et al. previously inferred extensive coupling between terminal and bridging modes on the basis of $^{34}S^{b}$ shifts observed in [2Fe–2S) proteins.[22]

3. Fe–S Stretching Modes. Stretching of the four bridging and four terminal Fe–S bonds account for eight modes, expected in the 240–450-cm^{-1} region. The classification of these coordinates is indicated in the last column of Table II for the ideal D_{2h} point group of the $Fe_2S_2{}^{b}S_4{}^{t}$ (S^{b}, S^{t} are bridging and terminal atoms) core of the complexes, as well as for the C_{2h} point group of the model with the ethanethiolate substituents. In this classification z is perpendicular to the $Fe_2S_2{}^{b}$ plane, x is along the Fe–Fe vector, and y is along the S–S vector. Consequently, the subscripts of the irreducible representations are permuted from those given by Yachandra et al.[4] who employed a different D_{2h} axis system. As demonstrated in the ensuing analysis, the D_{2h} selection rules hold quite well, permitting the lowering to C_{2h} symmetry to be applied as a perturbation.

(22) Meyer, J.; Moulis, J.-M.; Lutz, M. *Biochim. Biophys. Acta* **1986**, *873*, 108–118.

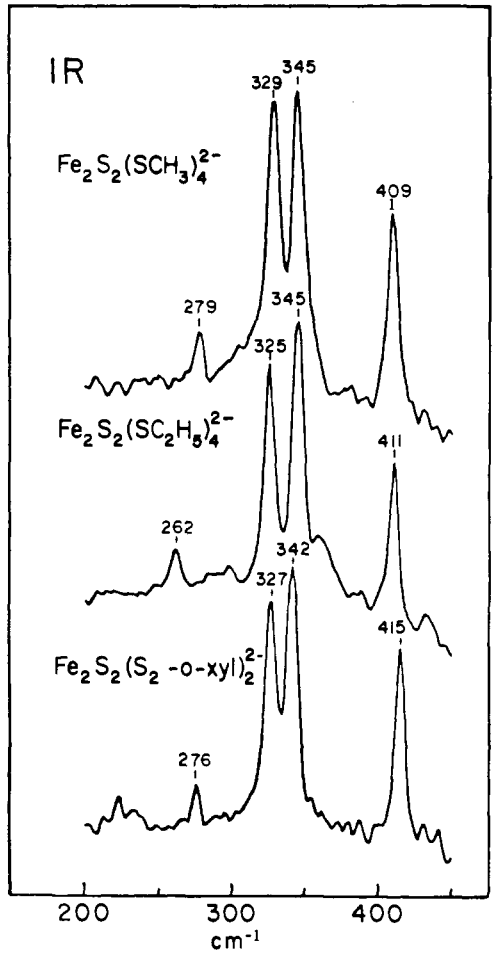

Figure 8. Low-temperature (77 K) infrared spectra in the Fe–S stretching region of the Fe_2S_2 salts (as Figure 2) in Nujol mulls: 200 scans; 4-cm^{-1} resolution.

Four of the Fe–S stretching modes are infrared active and four are Raman active, the center of symmetry assuring mutual exclusion. The infrared spectra (Figure 8) of the three analogue complexes are very clean in the region of interest, and show the four expected ^{34}S-sensitive bands. The isotope shifts, given in Table II, clearly mark the 415- and 327-cm^{-1} bands as bridging and terminal modes, respectively, while the 342- and 276-cm^{-1} bands display a mixed pattern, the former showing a somewhat smaller, and the latter a somewhat larger terminal ^{34}S shift. This mixing of the coordinates identifies the latter two modes as of B_{3u} symmetry (directed along the x axis), to which both bridging and terminal Fe–S stretching coordinates contribute (Table II). The 415-cm^{-1} band is the B_{2u} mode, which has no terminal contribution in D_{2h} symmetry. A terminal contribution is allowed in C_{2h} symmetry (B_{2u}, $B_{3u} \rightarrow B_u$), but the very small $^{34}S^t$ shift is a measure of the weakness of the perturbation. The 327-cm^{-1} band is the B_{1u} mode, which has no bridging contribution (in either D_{2h} or C_{2h} symmetry). Thus the isotope shifts provide unambiguous assignments of the infrared bands. We remark on the low intensity of the 276-cm^{-1} band, which we associate with the zero ^{54}Fe isotope shift (Table II). This mode can be described (see Figure 9) as an out-of-phase breathing motion of the two connected FeS_4 tetrahedra. The bond dipole changes therefore effectively cancel, leaving only a small overall transition dipole moment. The strong 327-, 342-, and 415-cm^{-1} bands show large ^{54}Fe shifts, 2–3 cm^{-1}. They involve concerted displacements of the Fe atoms, in the z, x, and y directions, respectively (Figure 9), and large net bond dipole changes.

RR spectra of the methanethiolate analogue complex (Figures 2 and 3) show two strong bands in the Fe–S stretching region, at 322 and 385 cm^{-1}. These are assigned to the two expected A_g modes in D_{2h} symmetry since totally symmetric modes are enhanced via the dominant A term resonance scattering mechanism.[23] The ~390-cm^{-1} band, common to all three analogues, shows a very small $^{34}S^t$ shift (Figure 5, Table II) in the xylenedithiolate complex, and is assigned to the A_g^b Fe_2S_2 ring breathing mode (Figure 9). The 322-cm^{-1}, A_g^t, band is sensitive to both $^{34}S^b$ and $^{34}S^t$ substitution and has mixed terminal and bridging character, the Fe atoms move away from each other while all the S atoms move toward the center. When 647.1-nm excitation is used (Figure 3 inset), another ^{34}S-sensitive band appears in the methanethiolate analogue RR spectrum, at 313 cm^{-1}. This is assigned to the B_{1g} (D_{2h}) mode, which is a purely bridging mode (Table III). This nontotally symmetric mode requires vibronic activation via the B resonance scattering term.[23] Evidently vibronic mixing is less important at 568.2 nm, where the 313-cm^{-1} band is not seen, than at 647.1 nm, probably because the absorption strength is higher at 568.2 nm and the A term is more dominant. (The vibronic coupling strength is no doubt also different for the different electronic states near these two wavelengths).

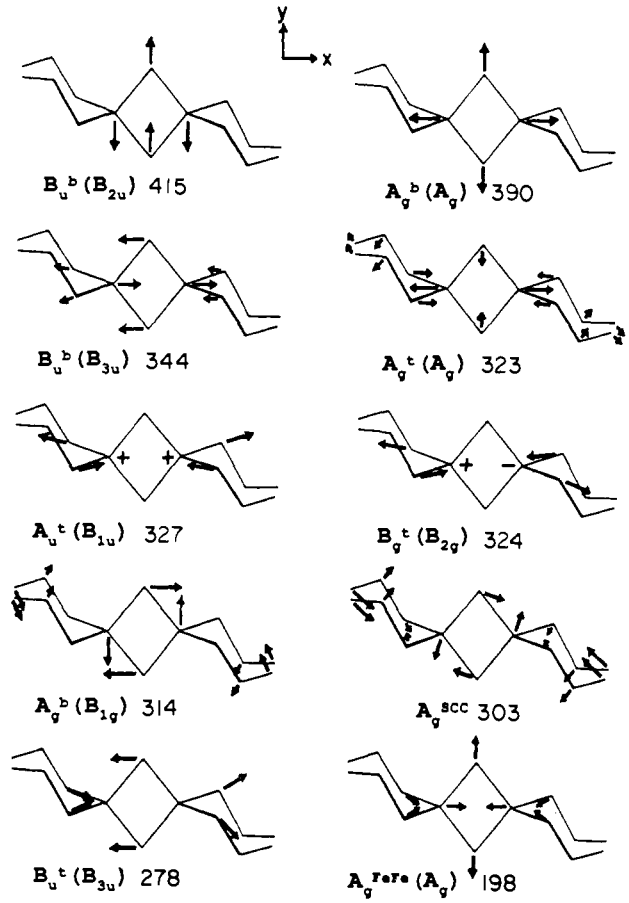

Figure 9. Eigenvectors for the normal modes (numbers are the calculated frequencies) involving Fe–S stretching, primarily, as well as the A_g modes involving S–C–C bending and the Fe–Fe displacement.

For the ethanethiolate and xylenedithiolate analogues, however, the ~313-cm^{-1} band *is* seen with 568.2-nm excitation (Figure 2), as is a nearby band at ~306 cm^{-1}, attributed to S–C–C bending (vide infra). The activation of the B_{1g} (D_{2h}) mode in these complexes is a manifestation of symmetry lowering, since the corresponding mode in the C_{2h} point group (Table II) has A_g symmetry, and is therefore subject to A term enhancement. Lower symmetry per se is insufficient, however, since the point group of the methanethiolate complex must also be lower than D_{2h}, unless the Fe–S–C angle is 180°; the crystal structure is not known, but Fe–S–C angles are always bent. The activation mechanism in the ethanethiolate and xylenedithiolate complexes is kinematic mixing of S–C–C bending character into the formally A_g Fe–S^b stretching mode, as discussed below.

(23) Clark, R. J. H.; Dines, T. J. *Angew. Chem., Int. Ed. Engl.* **1986**, *26*, 131–158.

For the ethanethiolate complex still another band is seen with 647.1-nm excitation (not shown), at 326 cm^{-1}, with an undetectable $^{34}S^b$ shift. This is assigned to the B_{2g} mode, which has a terminal but no bridging contribution; it becomes B_g in the C_{2h} point group (Table III) and cannot be activated via the A term. The frequency is expected to be essentially the same as that of the B_{1u} IR band (325 cm^{-1} observed) because these two terminal modes differ only in the phases of the Fe–S^t stretches on opposite sides of the $Fe_2S_2^b$ ring (Figure 9). This assignment completes the list of eight Fe–S stretches. In the previous study[4] the Raman modes, B_{1g} (313 cm^{-1}), A_g (323 cm^{-1}), and B_{2g} (324 cm^{-1}) were misassigned because of the unavailability of isotope shifts and the somewhat lower quality spectra.

4. Fe–S Bending and the Fe–Fe Stretching Mode. The xylenedithiolate complex RR spectrum has a strong band at 197 cm^{-1} with a substantial (1.5 cm^{-1}) ^{54}Fe isotope shift (Table II). The methanethiolate and ethanethiolate analogues show corresponding bands at 210 and 205 cm^{-1}, although the intensity is low for the ethanethiolate complex. This band is assigned to an A_g mode having a large relative displacement of the Fe atoms (Figure 9). This assignment naturally raises the question of the extent of Fe–Fe bonding in these species. The Fe–Fe distance in the xylenedithiolate complex, 2.698 Å,[3] is long for a bond but short for a nonbonded contact. The Fe^{3+} ions are antiferromagnetically coupled and the ground state is diamagnetic,[16] but coupling pathways are available via the bridging S^{2-} ions as well as by direct overlap of the Fe orbitals. Electronic structure calculations[16] indicate a significant direct overlap. The mode frequency, 200 cm^{-1}, is in the region where metal–metal stretching modes are commonly observed,[24] but the frequency itself is not an indication of the metal–metal bond strength in bridged polynuclear complexes because the metal–metal displacement is the resultant of all the forces in the ring (cyclic redundancy).[18] The ~200-cm^{-1} frequency can be calculated with a force-field that includes a Fe–Fe stretching constant (ref 4) or one that has instead a Fe···Fe nonbonded constant (present work), and both of these could be set to zero if the S–Fe–S angle bending constants were readjusted, albeit not to physically satisfactory values (as indicated by trial calculations).

The substantial intensity of the Fe–Fe mode does suggest a significant Fe–Fe interaction, however. In nonresonance Raman studies of bridged polynuclear complexes, this relationship has been quantified by calculating a metal–metal bond polarizability derivative.[25] Relatively weak bonds were found to give large intensities because of the expected dependence of the polarizability derivative on the cube of the bond distance. In RR scattering the intensity is a complex function of the excited-state potential surface, the resonance detuning interval and a variety of interference effects.[26] Nevertheless, the observation of strong scattering, at least in the xylenedithiolate complex, indicates a large Franck–Condon product for a mode that involves the Fe–Fe displacement primarily. The implied dependence of the excited-state wave function on the displacement suggests nonnegligible mutual overlap of the Fe orbitals.

The xylenedithiolate complex RR spectrum shows three other ^{34}S-sensitive low-frequency bands, at 165, 146, and 139 cm^{-1}. We assign the 165-cm^{-1} band, which does not shift upon $^{34}S^b$ substitution (Figure 5) to an internal mode of the ligand. The 146- and 139-cm^{-1} bands are close to the frequencies, 150 and 130 cm^{-1}, assigned to Fe–S bending modes in the 1-Fe protein, rubredoxin,[27] and are similarly assigned to S^b–Fe–S^t modes in the xylenedithiolate complex. The methanethiolate and ethanethiolate complexes show single RR bands at 120 and 117 cm^{-1}, which may have a similar origin. The frequency lowering relative to the xylenedithiolate complex may reflect the freeing of the xylenedithiolate chelate ring constraint in the methanethiolate and ethanethiolate complexes.

Reasonable candidates for the 146- and 139-cm^{-1} modes are found in the normal coordinate analysis, but 12 other modes are calculated in the 50–160-cm^{-1} region. Consequently the low-frequency part of the force field is undetermined.

5. Raman Activity of the 276-cm^{-1} IR Band and Its Overtone. Mutual exclusion breaks down in the xylenedithiolate complex RR spectra (Figure 5), which shows appreciable activation of the 277-cm^{-1} B_{3u} IR mode (clearly identifiable via its isotope shifts). This Raman activation requires a loss of the molecular symmetry center. While the xylenedithiolate complex crystal structure shows C_i site symmetry,[3] it is possible that the microcrystalline material prepared in this experiment had a different crystal packing. Alternatively, the asymmetry may have been induced by the sample preparation procedure, which involved grinding and pressing with KBr. The 277-cm^{-1} B_{3u} mode is weaker in the methanethiolate analogue RR spectra and is not seen at all for the ethanethiolate complex, implying a smaller environmental asymmetry in these samples.

More arresting than the RR activation of the 277-cm^{-1} B_{3u} fundamental is the finding of an even stronger overtone band in the xylenedithiolate complex RR spectrum (Figures 2 and 6). The 554-cm^{-1} band is clearly established as the overtone of the 277-cm^{-1} band by its isotope shifts. The overtone (and all even-quantum transitions) is Raman-allowed, even if the fundamental is not (e.g., $B_{3u} \times B_{3u} = A_g$). For a nontotally symmetric mode, however, overtone RR intensity requires a force constant change in the resonant excited state (change in the potential surface curvature).[23] In the present instance the excited-state force constant change is evidently linked to the environmental asymmetry since the intensity of the corresponding 557-cm^{-1} overtone for methanethiolate is lower than in the xylenedithiolate complex, as is that of the 279-cm^{-1} fundamental (Figure 2), while both the overtone and the fundamental are absent for the ethanethiolate complex.

We suggest that this remarkable behavior of the 277-cm^{-1} mode and its overtone is rooted in the character of the normal mode. As noted above in connection with the low IR intensity, this mode is basically a concerted out-of-phase breathing motion of the linked FeS_4 tetrahedra. The Fe–S bonds are stretched on one side of the dimer and contracted on the other side. Such a mode would be expected to have a large Raman polarizability were it not for the phase cancellation. Indeed its frequency is close to that of the breathing mode, 297 cm^{-1}, of the monomeric tetrahedral complex $[Fe(S_2\text{-}o\text{-}xyl)_2]^-$, which produces the strongest band in the RR spectrum.[11] Consequently, small asymmetric environmental effects could lead to significant RR intensity of the fundamental. The excited-state potential for this mode might be even more sensitive to an asymmetric environment, since in such an environment a one-photon CT transition could produce a charge-localized state (Fe^{2+} on one side, Fe^{3+} on the other) and thereby lower the force constant for the out-of-phase breathing mode under consideration. The sensitivity of the 277-cm^{-1} band to environmental asymmetry accounts for its astonishingly large RR intensity in Fe_2S_2 proteins, as discussed further in the succeeding paper.[8]

6. Other Overtone and Combination Bands: ν_{C-S}. The 500–800-cm^{-1} region of the xylenedithiolate complex RR spectra (Figure 6) shows other weak bands assignable to overtones and combinations of the Fe–S stretching Raman fundamentals. The possible two-quantum transitions are indicated in Figure 6 and listed in Table IV where they are matched to the observed bands. To a first approximation, the intensities of overtones and combinations should be proportional to the squares and products of the corresponding fundamentals.[28] Deviations from this rule reflect changes in excited-state force constants and mode compositions (Duschinsky rotation).[29] A marked deviation is seen

(24) (a) Kubas, G. J.; Spiro, T. G. *Inorg. Chem.* **1973**, *12*, 1797–1801. (b) Scovell, W. M.; Spiro, T. G. *Inorg. Chem.* **1974**, *13*, 304–308. (c) Kettle, S. F. A.; Stanghellini, P. L. *Inorg. Chem.* **1977**, *16*, 753–758. (d) Butler, I. S.; Kishner, S.; Plowman, K. R. *J. Mol. Struct.* **1978**, *43*, 9–15.

(25) Spiro, T. G. *Prog. Inorg. Chem.* **1970**, *11*, 1–51.

(26) Mortensen, O. S.; Hassing, S. *Adv. Infrared Raman Spectrosc.* **1979**, *6*, 1–60.

(27) Czernuszewicz, R. S.; LeGall, J.; Moura, I.; Spiro, T. G. *Inorg. Chem.* **1986**, *25*, 696–700.

(28) (a) Heller, E. J. *Acc. Chem. Res.* **1981**, *14*, 368. (b) Heller, E. J.; Sundberg, R. L. *J. Phys. Chem.* **1982**, *86*, 1822.

Table IV. Combination Bands and Isotope Shifts[a] (cm^{-1}) in the 568.2-nm Excited RR Spectra of $(Et_4N)_2[Fe_2S_2(S_2\text{-o-xyl})_2]$

expected combinations						observed bands			
ν_1	ν_2	$\nu_1 + \nu_2$	$\Delta^{34}S^b$	$\Delta^{34}S^t$	$\Delta^{54}Fe$	ν	$\Delta^{34}S^b$	$\Delta^{34}S^t$	$\Delta^{54}Fe$
306 + 197		503	3.5	3.4	2.5				
313 + 197		510	4.2	3.7	3.2				
323 + 197		520	3.0	6.5	2.5				
276 + 276		552	6.4	10.4	0.0	554	6	9	0
391 + 197		588	6.9	2.9	4.2	587	5	0	3
306 + 306		612	5.0	2.0	2.0				
313 + 306		619	5.7	2.3	2.7	617	5	6	3
313 + 313		626	6.4	2.6	3.4				
323 + 306		629	4.5	5.1	2.0				
323 + 313		636	5.2	5.4	2.7				
323 + 323		646	4.0	8.2	2.0				
391 + 306		697	8.4	1.5	3.7	696	8	3	2.5
391 + 313		704	9.1	1.8	4.4				
391 + 323		714	7.9	4.6	3.7	713	8	5	3
391 + 391		782	11.8	1.0	5.4	780	9	1	5

[a] See footnote *b* of Table II.

in the xylenedithiolate complex spectra. Since the trio of fundamentals at 306, 313, and 323 cm^{-1} have about the same intensity, comparable enhancement is expected for all six overtones and combinations, but only a single band is seen at 617 cm^{-1}, corresponding to the (306 ± 313)-cm^{-1} combination. This selectivity probably reflects a Duschinsky rotation among these three closely spaced modes, which are kinematically coupled (vide infra) in the ground state. Moreover, the 617-cm^{-1} band shows the predicted $^{34}S^b$ shift, but too large a $^{34}S^t$ shift, 6 versus 2.3 cm^{-1} calculated for the (306 + 313)-cm^{-1} combination. This can be attributed to an altered selectivity in the $^{34}S^t$ molecule, this time for the (306 + 306)-cm^{-1} overtone (predicted at 612 versus 611 cm^{-1} observed), reflecting a $^{34}S^t$ effect on the Duschinsky rotation. On the other hand, the combinations of these three bands with the 391-cm^{-1} fundamental (696–715 cm^{-1}) show nearly the expected intensity pattern, although the middle band is not clearly resolved. It is reasonable that intensity disparities produced by Duschinsky rotation would appear more strongly among mutual combinations of the rotated modes than among their combinations with an unaffected mode.

The band observed at 676 cm^{-1} does not correspond to any combination. It is in the region (650-750 cm^{-1}) where C–S stretching modes are expected, and it shows the proper $^{34}S^t$ (3 cm^{-1}). Therefore it is assigned to $\nu_{C\text{-}S}$. There are actually four C–S stretching modes, but the C–S bonds are separated by at least two Fe–S bonds, and differential coupling is expected to be small. The four C–S stretches (A_g, B_g, A_u, B_u) are calculated at the same frequency, 673 cm^{-1}, with $^{34}S^t$ shifts of 5.1 cm^{-1}. The ligand itself, $(HS)_2$-o-xyl, has a strong Raman band at 669 cm^{-1} which shifts down by 42 cm^{-1} upon methylene deuteration (calculated downshift is 31 cm^{-1}). A substantially higher frequency, ~750 cm^{-1}, was assigned to $\nu_{C\text{-}S}$ in "blue" Cu proteins, which has a cysteinate group bound to Cu^{2+}.[30] The frequency elevation is attributed to coupling with Cu–S stretching, whose frequency is unusually high, ~400 cm^{-1}. In the $Fe_2S_2(SR)_4$ complexes the terminal Fe–S stretches are in the ~300-cm^{-1} region and the coupling with $\nu_{C\text{-}S}$ is therefore smaller.

7. S–C–C Bending Mode. As noted above, the xylenedithiolate and ethanethiolate complexes have an extra band at 306 cm^{-1}, which is assigned to S–C–C bending, a coordinate which is absent in the methanethiolate complex. The S–C–C mode is coupled to the neighboring $B_{1g}{}^b$ and $A_g{}^t$ modes at 313 and 323 cm^{-1} (317 and 331 cm^{-1} for the ethanethiolate complex). Direct evidence for this coupling can be seen in the ^{34}S shift pattern. The $^{34}S^b$ shifts of the $B_{1g}{}^b$ and $A_g{}^t$ modes are measurably larger in the methanethiolate complex (3.9, 2.6 cm^{-1}) than in the ethanethiolate (3.7, 1.0 cm^{-1}) or xylenedithiolate (3.2, 2.0 cm^{-1}) complexes, while the additional 306-cm^{-1} band shows a sizable $^{34}S^b$ shift, 1.7 and 2.5 cm^{-1} for the ethanethiolate and xylenedithiolate complexes. Thus the $^{34}S^b$ shift belonging to the $B_{1g}{}^b$ and $A_g{}^t$ modes is shared with the $A_g{}^{SCC}$ mode. The frequency, 306 cm^{-1}, is considered reasonable for δ_{SCC}, since this mode has been assigned at 330 cm^{-1} in C_2H_5SH.[31]

In order to be quite sure of the δ_{SCC} assignment we examined the RR spectrum of the d_8 isotopomer and the d_8, $^{34}S^b$ doubly labeled isotopomer, with the idea that the S–C–C bending frequency should be sensitive to deuteration at the carbon atom adjacent to the sulfur. Figure 7 compares the relevant portions of these spectra with those of the h_8 and h_8, $^{34}S^b$ species. A dramatic change is seen upon deuteration, which can be interpreted according to the band correlations indicated by the arrows in the figure. The 323-cm^{-1} $A_g{}^t$ band shifts down substantially, to 316 cm^{-1}. This downshift reveals a weak band at 331 cm^{-1}, observable as a shoulder in the h_8 spectrum, which is tentatively assigned to the $B_{2g}{}^t$ mode (seen at 326 cm^{-1} with 647.1-nm excitation in the ethanethiolate complex). The 313-cm^{-1} $B_{1g}{}^b$ band shifts down only 1 cm^{-1} but doubles its relative intensity and increases its $^{34}S^b$ isotope shift (4.8 versus 3.2 cm^{-1}, Table II). At the same time the 306-cm^{-1} $A_g{}^{SCC}$ band disappears. We infer that this band gains all of its intensity in the h_8 spectrum by mixing with the $B_{1g}{}^b$ mode, and loses it in the d_8 spectrum when it shifts away, by an undetermined amount; conversely the $B_{1g}{}^b$ band increases its intensity and isotope shift when it is unmixed in the d_8 species. (An opposite effect is seen in the h_8, $^{34}S^b$ spectrum where the $B_{1g}{}^b$ band loses more intensity to the $A_g{}^{SCC}$ band as the mixing is increased, the frequency separation decreasing slightly.) We attempted to model the deuteration shifts by introducing C–H bonds at the methylene positions in the calculation. This calculation gave the correct d_8 and $^{34}S^b$ shift, for the $B_{1g}{}^b$ mode, and predicted a 5-cm^{-1} d_8 downshift for $A_g{}^{SCC}$. The calculated downshift of the $A_g{}^t$ mode (2 cm^{-1}) was too small, however.

It is remarkable that in the unmixed state (d_8 species) the $B_{1g}{}^b$ intensity is greater than the $A_g{}^t$ intensity, although it is vanishingly small for the methanethiolate complex, showing up only with 647.1-nm excitation. Despite the unmixing of the Ag^{SCC} mode, strong A_g character must be induced into the $B_{1g}{}^b$ mode by the presence of the SCC units in the xylenedithiolate complex; one can presume that this holds true as well for the ethanethiolate complex from the similar intensity pattern in the h_8 species.

8. Influence of the Fe–S–C–C Dihedral Angle. The occurrence of the S–C–C bending frequency in the range of the Fe–S stretching frequencies means that the Fe–S–C–C dihedral angle (τ) is an important determinant of the normal modes. When this angle is 180°, then the S–C–C bend and Fe–S stretch are in line and coupling between them is maximal, whereas the coupling is minimized when the angle is 90°. This angular dependence is also seen for disulfides, the S–S stretch being dependent on the S–S–C–C dihedral angle,[32] even though ν_{SS} (~500 cm^{-1}) is much higher than δ_{SCC}. The influence is expected to be much stronger for Fe–S stretching, because the frequencies are similar. Large effects were found in model calculations for mononuclear $[Fe(SR)_4]^-$ complexes,[11] although the S–C–C bending force constant was not known precisely. In the present case this force constant is known because of the near coincidence and consequent mixing of the $A_g{}^{SCC}$ and $B_{1g}{}^b$ modes, as discussed above. Consequently, the dependence on dihedral angle can be analyzed with confidence.

In the xylenedithiolate complex τ is 90°, and the S–C–C/Fe–S bend–stretch interaction is actually at a minimum. Figure 10 shows the effect of increasing this angle synchronously for all four ethanethiolate groups in the model, maintaining the overall C_{2h} point group. The four panels separate the four symmetry blocks, each of which contains one of the four S–C–C bending modes; only the $A_g{}^{SCC}$ mode is observed in the RR spectra. As the

(29) Blair, D. F.; Campbell, G. W.; Schoonover, J. R.; Chan, S. I.; Gray, H. B.; Malmstrom, B. G.; Pecht, I.; Swanson, B. I.; Woodruff, W. H.; Cho, W. K.; English, A. M.; Fry, H. A.; Lum, V.; Norton, K. A. *J. Am. Chem. Soc.* **1985**, *107*, S755.

(30) (a) Nestor, L.; Reinhammar, B.; Spiro, T. G. *Biochim. Biophys. Acta* **1986**, *869*, 286–292. (b) Ferris, M. S.; Woodruff, W. H.; Tennent, D. L.; McMillen, D. R. *Biochem. Biophys. Res. Commun.* **1979**, *88*, 288.

(31) Durig, J. R.; Bucy, W. E.; Wurrey, C. J.; Carreira, L. A. *J. Phys. Chem.* **1975**, *79*, 988–993.

(32) Sugeta, H.; Go, A.; Miyazawa, T. *Chem. Lett.* **1972**, *83*, 86.

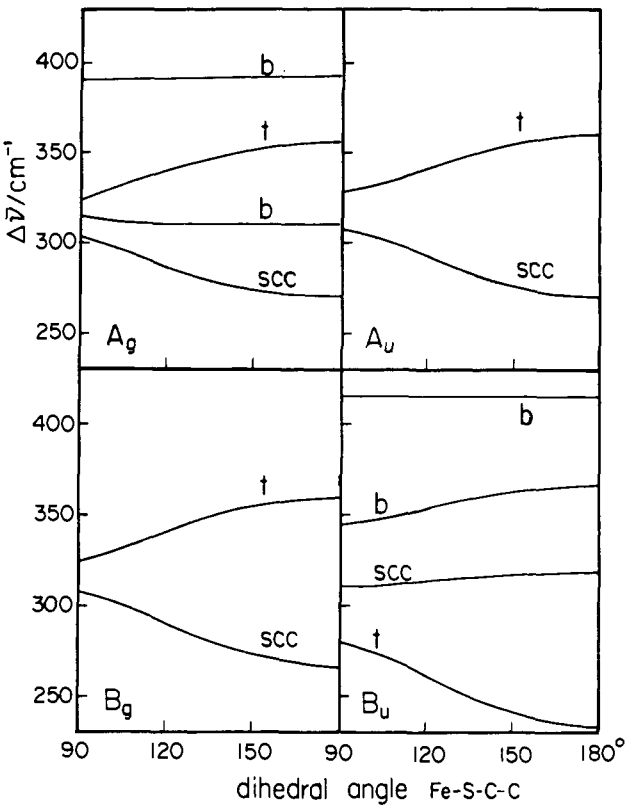

Figure 10. Calculated mode frequencies as functions of the Fe–S–C–C dihedral angle, shown separately for the four C_{2h} symmetry blocks. The modes are labeled according to the main internal coordinate contributor, bridging (b) or terminal (t) Fe–S bond stretching, or S–C–C bending (SCC). The force constants are given in Table I.

dihedral angle increases, the A_g^{SCC} mode decreases from 306 toward 270 cm^{-1} while the A_g^t mode increases from 323 toward 350 cm^{-1}, reflecting the expected interaction between S–C–C bending and terminal Fe–S stretching. The 313-cm^{-1} A_g^b mode is scarcely affected, however, the weak coupling reflecting its B_{1g}^b (in D_{2h} symmetry) parentage and largely bridging character. The 391-cm^{-1} A_g^b mode, being nearly purely bridging in character, is essentially unaffected by τ. The A_u and B_g blocks contain only terminal Fe–S stretches, which are nearly degenerate because of the small trans-bridge coupling, as discussed above. Both of them increase in frequency, with increasing τ, paralleling the A_g^t mode, while the S–C–C bending modes decrease.

A quite different pattern is seen for the B_u block because the starting (90°) frequency of the terminal mode is lower than that of S–C–C bend. The former mode decreases in frequency with increasing τ, in contrast to all the other Fe–S stretches. The 342-cm^{-1} B_u^b mode increases somewhat because it has substantial terminal as well as bridging character. The result of these two opposed couplings is to leave the S–C–C bending mode frequency nearly unaltered in this block. The 415-cm^{-1} B_u^b mode, being purely bridging in character, does not couple.

Trial calculations were also carried out in which τ was varied independently for two of the ethanethiolate groups at a time. The resulting frequencies were intermediate between those calculated when all four angles had one value or the other; of course, the symmetry labels are altered in this situation, and there are some additional mode mixings. But the general prediction remains that rotating the Fe–S–C–C units about one or more of the S–C bonds from 90° toward 180° results in an increase of the three terminal modes above 300 cm^{-1}. This expected pattern helps to account for variations among the Fe_2S_2 protein spectra, as discussed in the succeeding article.[8]

Conclusions

The eight Fe–S stretching modes are completely assigned in RR and IR spectra of the methanethiolate, ethanethiolate, and xylenedithiolate Fe_2S_2 analogue complexes via their activities and ^{34}S and ^{54}Fe isotope shifts. These modes show substantial coupling between terminal and bridging Fe–S stretches. One of the S–C–C bending modes is also assigned in the ethanethiolate and xylenedithiolate RR spectrum, its near coincidence and consequent interaction with one of the Fe–S stretching modes allowing a precise calculation of the S–C–C bending force constant. A physically reasonable force field has been developed which permits accurate calculations of all eight Fe–S stretching modes, and the S–C–C bending mode, as well as their isotope shifts. This force field is used to gauge the sensitivity of the vibrational frequencies to the Fe–S–C–C dihedral angle (τ); as τ increases from 90°, four of the Fe–S stretching modes increase, while one decreases, owing to differential couplings with the S–C–C bending coordinates.

The lowest frequency Fe–S stretching mode, at ~275 cm^{-1}, has B_u symmetry, but is readily activated in the RR spectra via asymmetric environmental perturbations; its overtone gains RR enhancement even more readily. These activations are explained by the out-of-phase breathing character of the mode, for which a large excited-state origin shift and force constant change is expected if the environment is asymmetric. Combination tone RR intensities also suggest Duschinsky rotation in the excited state among the interacting S–C–C and Fe–S modes.

A RR band at ~200 cm^{-1} is identifiable with the Fe–Fe mode, involving mutual displacement of the Fe atoms. While the restoring force for this mode is a collective property of the atoms in the Fe_2S_2 ring, the strong scattering, at least in the case of the xylenedithiolate complex, requires a substantial excited-state origin shift and suggests an appreciable direct interaction of the Fe orbitals. RR bands in the 120–150-cm^{-1} region are assigned to S–Fe–S bending modes.

Acknowledgment. This work was supported by NIH Grant GM13498 (to T.G.S.).